

Dual-Ligand Eu-MOF for Ratiometric Fluorescence Sensing and Visual Detection of Fluoride Ions

Wen-Zhe Chen, Ting-Ting Xiao, Lin-Lin Wang, Min Zhang*, Xue-
Bo Yin*

Institute for Frontier Medical Technology, College of Chemistry and Chemical Engineering, Shanghai

University of Engineering Science, Shanghai 201620, China

**Email: xbyin@nankai.edu.cn; zhangmin@sues.edu.cn*

Contents

Figure S1. The emission and excitation spectra of (A) Eu-AIP, (B) Eu-BDC,(C) Eu-AIP/BDC, (D) The UV-vis spectra of the 5-AIP (black line), H₂BDC(red line) and the Eu-AIP/BDC(blue line).

Figure S2. The thermogravimetric analysis (TGA) of Eu-AIP/BDC.

Figure S3. The response time of Eu-AIP/BDC to F⁻.

Figure S4. The fluorescence spectra and PXRD patterns of Eu-AIP/BDC after being dispersing in water for different time ($\lambda_{ex}=280$ nm).

Figure S5. The fluorescence spectra and PXRD patterns of Eu-AIP/BDC with pH 5.0 - 10.0 ($\lambda_{ex}=280$ nm).

Figure S6. Relationship between the polarity index of different solvents and the fluorescence intensity of the two emission centers.

Figure S7. The relationship between different water content and the emission intensity of Eu-AIP/BDC at 616 nm. ($\lambda_{ex}=280$ nm).

Table S1. The calculation of LOD. σ is approximately equal to the slope of the calibration curve; s is the standard deviation for N parallel blank solutions.

Figure S8. Fluorescent experiments of Eu-AIP/BDC in samples: emission spectra (A) and ratio col (B) of reference with different concentration F⁻; emission spectra (C) (E) and ratio column (D) (F) of the toothpaste with and without F⁻.

Figure S9. Fluorescent experiments of Eu-AIP/BDC in samples: emission spectra (A)

and ratio col (B) of River water with and without F^- ; emission spectra (C) and ratio column (D) of the Tap water with and without F^- ; emission spectra (E) and ratio column (F) of the Purified water with and without F^- .

Figure S10. The PRXD of Eu-AIP/BDC treated with F^- ions before and after.

Table S2. Comparing the performance of various systems of fluorescent probes for F^- in terms of response time and detection limit.

Results and Discussions

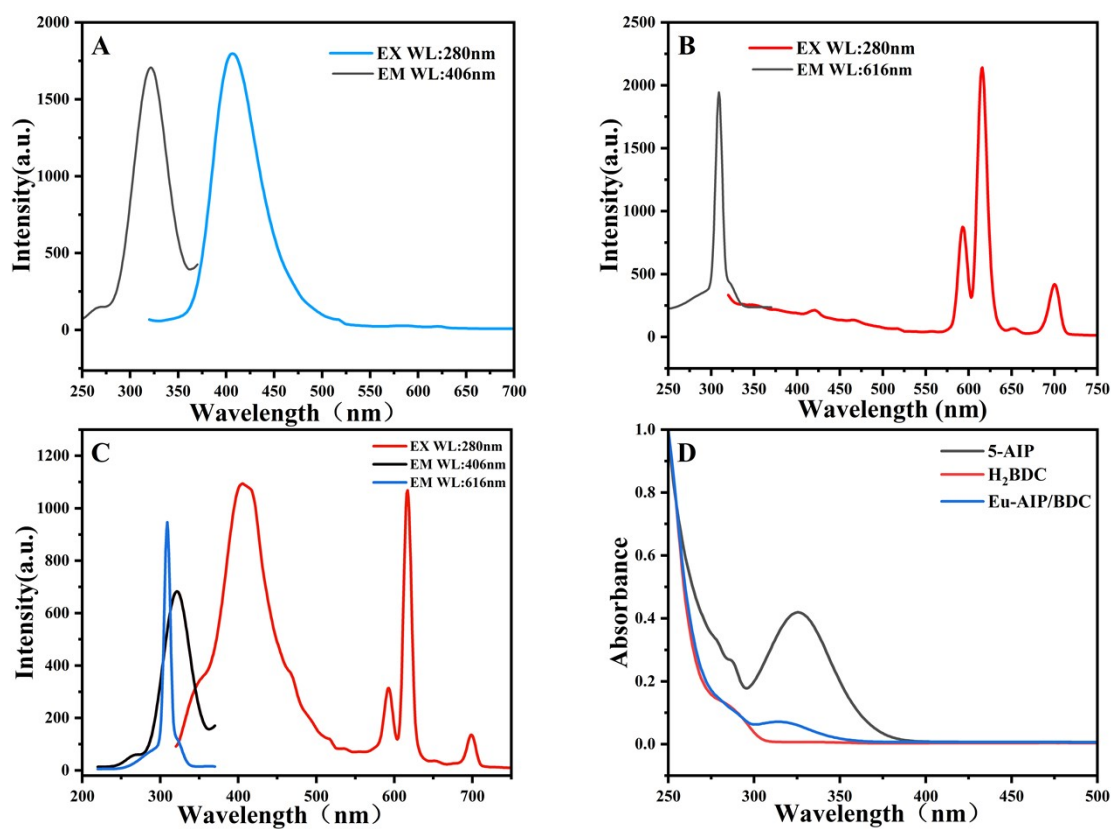


Figure S1. The emission and excitation spectra of (A) Eu-AIP, (B) Eu-BDC, (C) Eu-AIP/BDC, (D) The UV-vis spectra of the 5-AIP (black line), H₂BDC (red line) and the Eu-AIP/BDC (blue line).

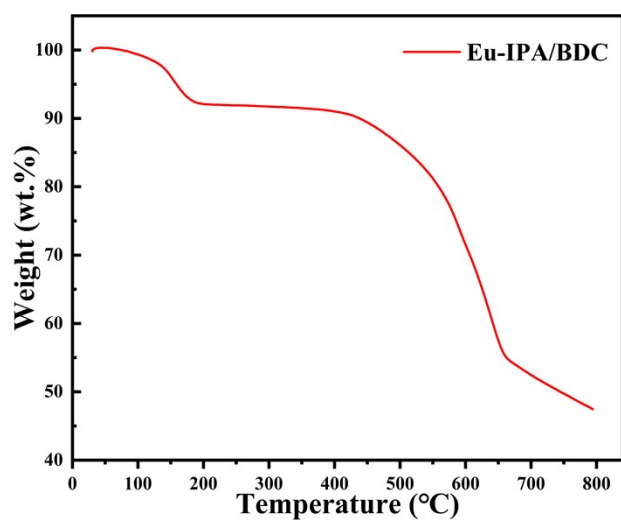


Figure S2. The thermogravimetric analysis (TGA) of Eu-AIP/BDC.

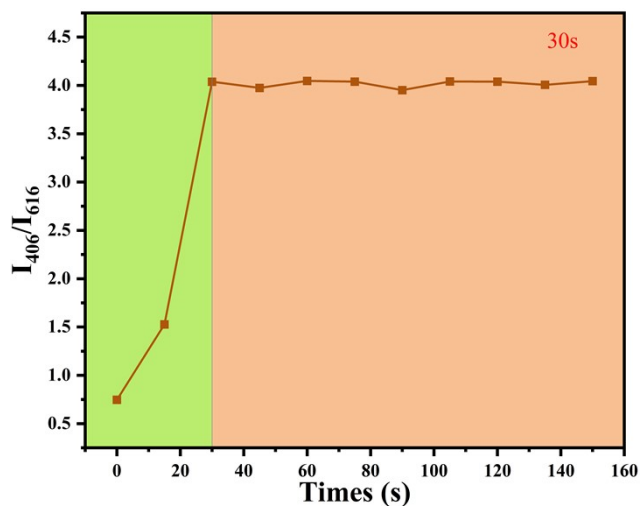


Figure S3. The response time of Eu-AIP/BDC to F^- .

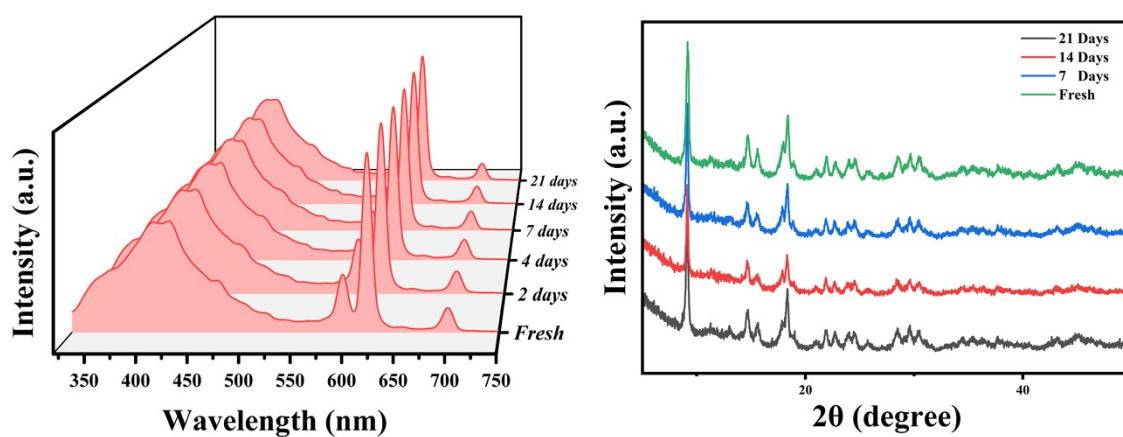


Figure S4. The fluorescence spectra and PXRD patterns of Eu-AIP/BDC after being dispersing in water for different time ($\lambda_{ex}=280$ nm).

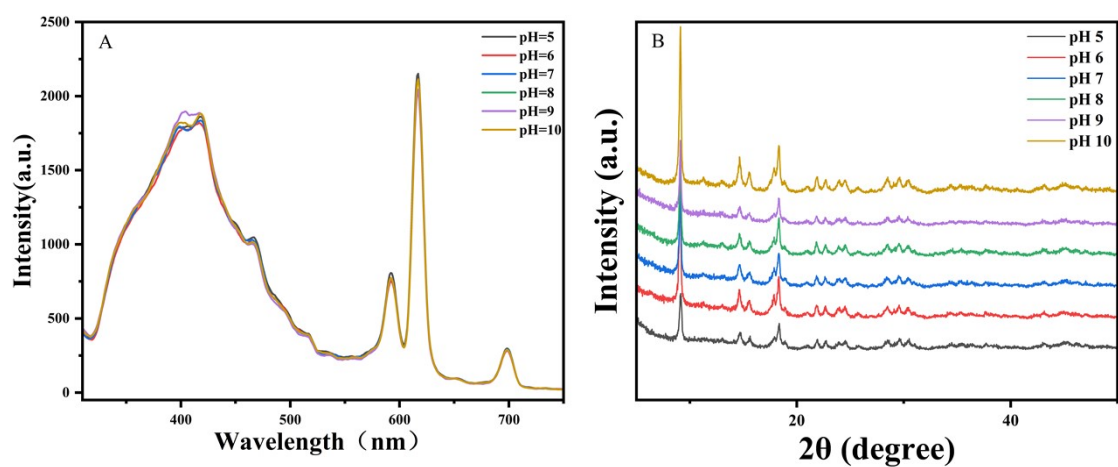


Figure S5. The fluorescence spectra and PXRD patterns of Eu-AIP/BDC with pH 5.0 - 10.0 ($\lambda_{ex}=280$ nm).

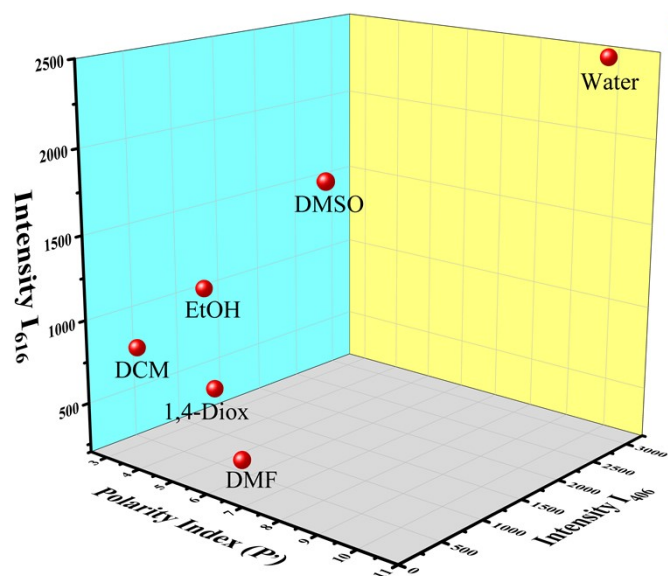


Figure S6. Relationship between the polarity index of different solvents and the fluorescence intensity of the two emission centers.

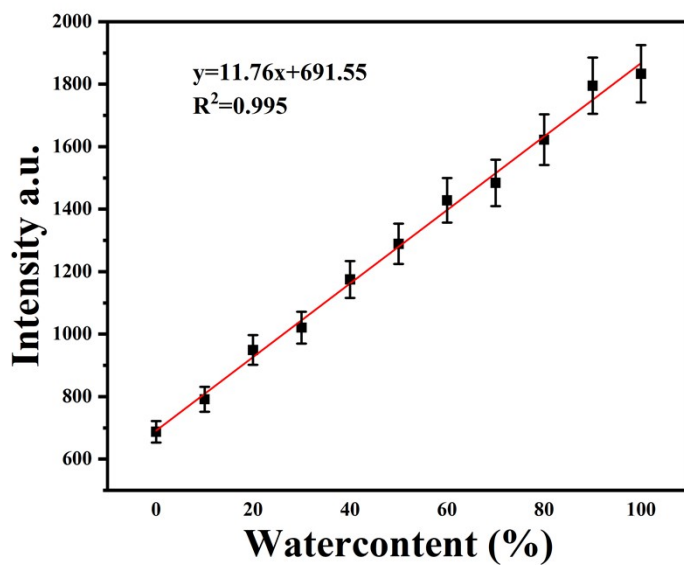


Figure S7. The relationship between different water content and the emission intensity of Eu-AIP/BDC at 616 nm. ($\lambda_{ex}=280$ nm).

Table S1. The calculation of LOD. σ is approximately equal to the slope of the calibration curve; s is the standard deviation for N parallel blank solutions

Formula	Blank signal			σ	s	D/ μM
	I ₄₀₆	I ₆₁₆	I ₄₀₆ /I ₆₁₆			
D = 3σ/s	1	1693	2582	0.655	0.0016	0.015
	2	1683	2551	0.659		
	3	1673	2543	0.657		

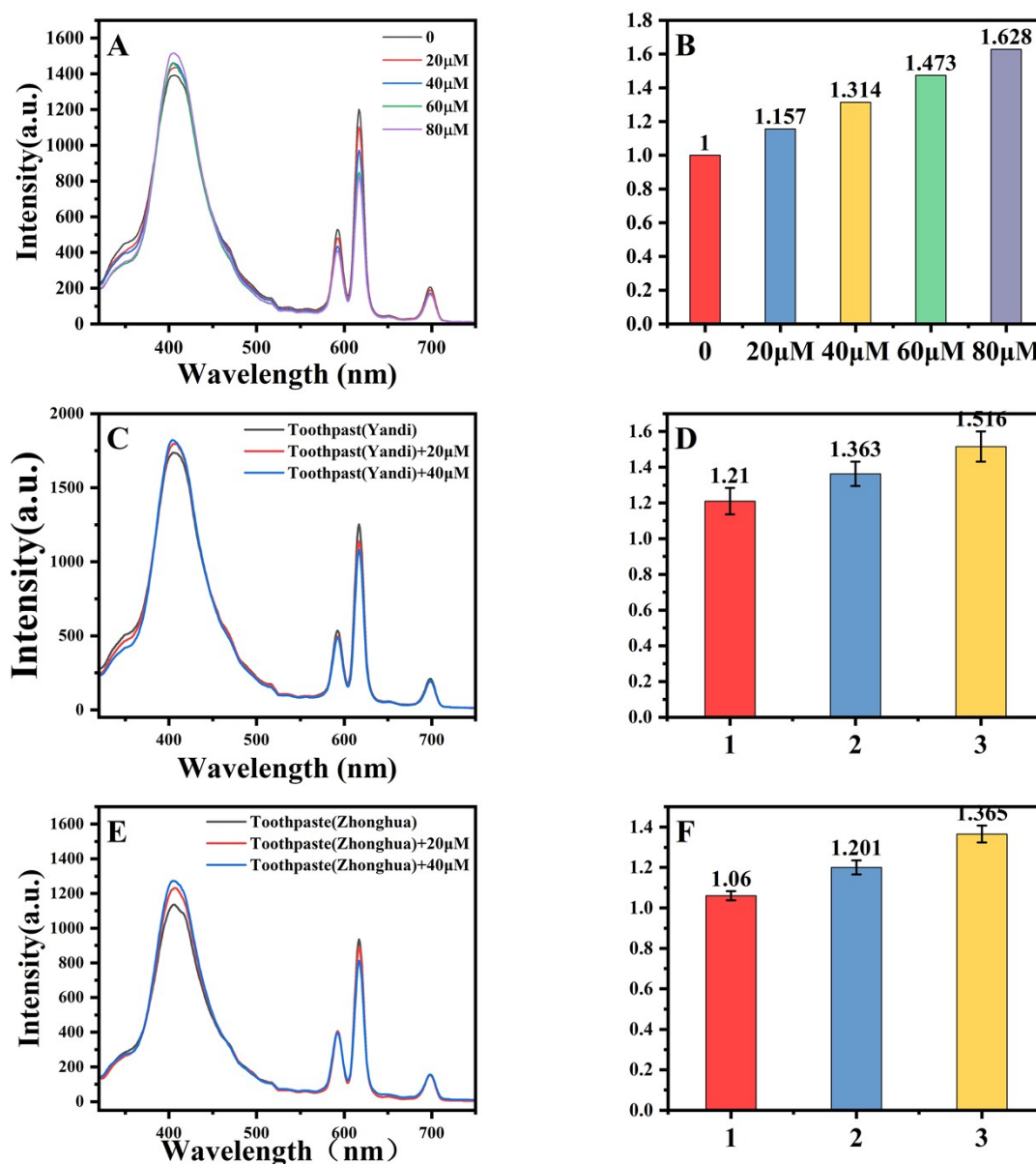


Figure S8. Fluorescent experiments of Eu-AIP/BDC in samples: emission spectra (A) and ratio column (B) of reference with different concentration F⁻; emission spectra (C) (E) and ratio column (D) (F) of the toothpaste with and without F⁻.

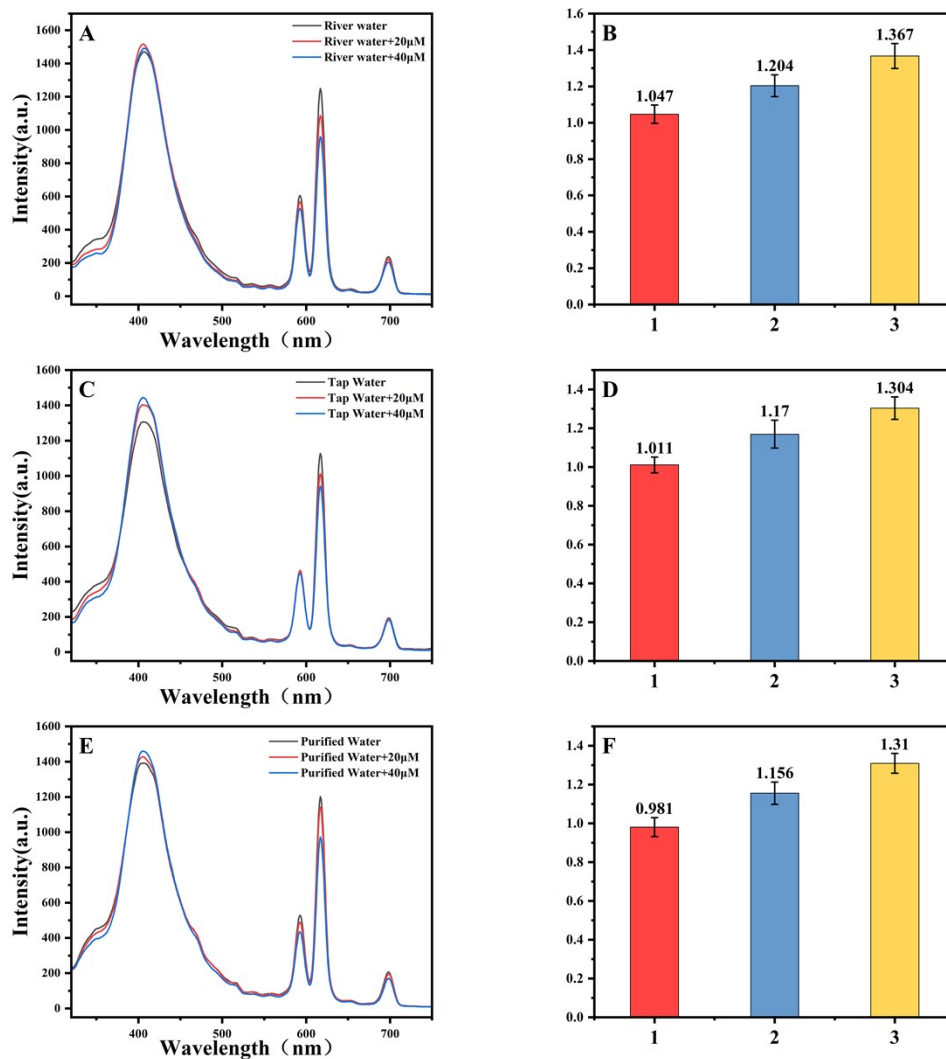


Figure S9. Fluorescent experiments of Eu-AIP/BDC in samples: emission spectra (A) and ratio column (B) of River water with and without F^- ; emission spectra (C) and ratio column (D) of the Tap water with and without F^- ; emission spectra (E) and ratio column (F) of the Purified water with and without F^-

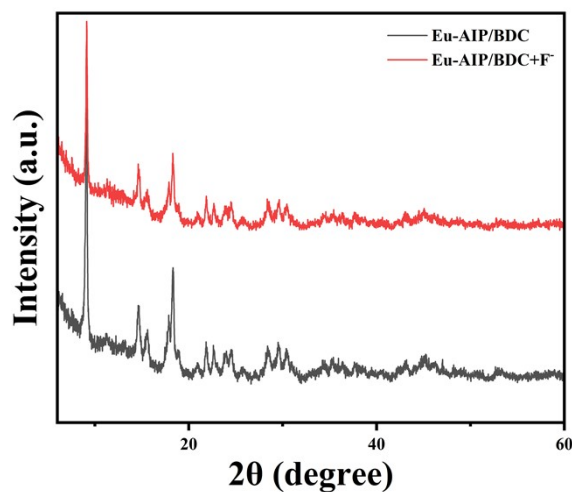


Figure S10. The PRXD of Eu-AIP/BDC treated with F^- ions before and after.

Table S2. Comparing the performance of various systems of fluorescent probes for F⁻ in terms of response time and detection limit.

MOF	Linear	LOD	Time	Visual detection	Ref
Eu-AIP/BDC	0–100 μ M	0.32 μ M	30s	yes	This work
Eu ³⁺ @UiO-66-IPA	50–250 μ M	0.22 μ M	-	yes	1
Zr-Mof	1–50 μ M	17.8 μ M	-	No	2
Tb ³⁺ @UIO66	0.1–0.6mM	4.02 μ M	>30s	yes	3
UiO-66 (NH ₂)-FITC	2–150 μ M	3.45 μ M	-	No	4
EuTPTC-NH ₂	0-5.12 mM	11.26 μ M	60s	No	5
UiO-66-NH ₂ @RhB	0-200 μ M	1.55 μ M	-	No	6
Eu-MOF	0–515 μ M	1.14 μ M	-	No	7
Tb/Eu(TATB)	0–45 μ M	2.30 μ M	30min	Yes	8
FS@UiO-66	0–0.4 mM	4.40 μ M	15min	No	9
Y-TCCP MOFs	1–200 μ M	0.25 μ M	3min	No	10

REFERENCES

- 1 J. Chen, T. Guo, H. Gao, T. He, J. Li, H. Li, X. Liu and A. Li, *ACS Applied Materials & Interfaces*, 2024, **16**, 60278–60287.
- 2 Y. Zhu, L. Zhu, W. Song and C. Deng, *Inorganic Chemistry Communications*, 2023, **154**, 110917.
- 3 J. Li, M. Liu, J. Li and X. Liu, *Talanta*, 2023, **259**, 124521.
- 4 Q. Li, H. Chen, S. You, Z. Lin, Z. Chen, F. Huang and B. Qiu, *Microchemical Journal*, 2023, **186**, 108318.
- 5 Amino-Functionalized Single-Lanthanide Metal–Organic Framework as a Ratiometric Fluorescent Sensor for Quantitative Visual Detection of Fluoride Ions | *Inorganic Chemistry*, <https://pubs.acs.org/doi/full/10.1021/acs.inorgchem.2c02533>, (accessed 21 January 2025).
- 6 M. Zhang, R. Liang, K. Li, T. Chen, S. Li, Y. Zhang, D. Zhang and X. Chen, *Spectrochimica Acta Part A: Molecular and Biomolecular Spectroscopy*, 2022, **271**, 120896.
- 7 H. Che, Y. Li, S. Zhang, W. Chen, X. Tian, C. Yang, L. Lu, Z. Zhou and Y. Nie, *Sensors and Actuators B: Chemical*, 2020, **324**, 128641.
- 8 X. Zeng, J. Hu, M. Zhang, F. Wang, L. Wu and X. Hou, *Anal. Chem.*, 2020, **92**, 2097–2102.
- 9 X. Zhao, Y. Wang, X. Hao and W. Liu, *Applied Surface Science*, 2017, **402**, 129–135.
- 10 X. Wang, C. Chu, Y. Wu, Y. Deng, J. Zhou, M. Yang, S. Zhang, D. Huo and C. Hou, *Sensors and Actuators B: Chemical*, 2020, **321**, 128455.